The Configuration of a Cable Towed in a Circular Path

RICHARD A. SKOP
U.S. Naval Research Laboratory, Washington, D.C.
AND
YOUNG-IL CHOO*
The Catholic University of America, Washington, D.C.

The problem of determining the equilibrium configuration of a cable towed in a circular path has both mathematical and practical interest. Mathematically, this interest is generated because of the multivalued nature of the boundary value problem. Practically, this interest arises because the towed drogue, for certain ranges of the governing parameters, obtains an equilibrium position very near the axis of rotation thus enabling pinpoint deliveries of payloads from fixed-wing aircraft. In this paper, the circular towing problem for a flexible, inextensible cable is examined. The equations of equilibrium and the boundary conditions which govern the cable configuration are derived and nondimensionalized to isolate the important parameters. The significance of these parameters for modeling the towing system is discussed. Finally, extensive numerical results are obtained for a particular airborne system. This example shows that an intimate relation exists between the mathematically interesting multivalued regions of solution and the practically interesting regions for which large towline verticality and small drogue radius are simultaneously present.

Introduction

IN three recent reports, Huang,[1] Choo,[2] and Skop[3] have considered the equilibrium configuration of a cable towed in a steady circular path. Huang, who restricted his calculations to an airborne system, was primarily interested in optimizing the verticality (ratio of vertical separation between towpoint and drogue to cable length) of the cable and did not comment on the ratio of drogue radius to towpoint radius; nor did he comment on the modeling properties of his equations. He did, however, report finding limited ranges of the governing system parameters for which multivalued equilibrium solutions existed. Choo, on the other hand, reported finding only single-valued solutions. However, his towing medium was water instead of air and this apparently limited the system parameters to the single-valued regions. Choo also did not consider the modeling properties of his equations. Skop restricted his numerical and experimental results to a vacuous towing medium and showed that multivalued solutions always existed if the cable length and the rotational frequency of the towpoint were above certain minimum values. Experimentally, he demonstrated that only one of these solutions was stable.

Aside from its intrinsic mathematical interest due to the multivalued nature of the boundary value problem, the circular towing concept also has practical usage. This is because the drogue, for certain values of the governing parameters, obtains an equilibrium position very near the axis of rotation. Thus, for example, a fixed-wing aircraft flying in a circular pattern could make pinpoint deliveries of payloads, or a ship moving in a circular path could make an intensive search of a particular underwater area.

In this paper, the circular towing problem for a flexible, inextensible cable is re-examined. The equations of equilibrium and the boundary conditions which govern the cable configuration are derived and nondimensionalized to isolate the important parameters. A discussion of these parameters and their significance for experimentally modeling the towing system follows. Finally, extensive numerical results are obtained for a particular airborne system. This example shows that an intimate relation exists between the mathematically interesting multivalued regions of solution and the practically interesting regions for which large towline verticality and small drogue radius are simultaneously present.

Received April 21, 1971. The authors wish to acknowledge the helpful advice and suggestions of Mario J. Casarella, The Catholic University of America, during the preparation of this paper.

* Research Associate, Institute of Ocean Science and Engineering.

Equations of Equilibrium

Let X, Y, and Z be the axes of a right-handed, Cartesian coordinate system (Fig. 1) which rotates along with the cable towpoint about the Z axis. Z is considered increasing in the antigravitational direction. The rate of rotation Ω is defined by the cable towpoint which moves along a circle of radius R at a speed V. Consequently, $\Omega = V/R$. The unit vectors along the X, Y, and Z axes are designated by $\mathbf{i}$, $\mathbf{j}$, and $\mathbf{k}$, respectively.

If the position vector of a point on the cable is denoted by $\mathbf{P}$, where

$$\mathbf{P} = X\mathbf{i} + Y\mathbf{j} + Z\mathbf{k}$$

then the equations of equilibrium for a flexible, inextensible cable are given by

$$d/dS(T'd\mathbf{P}/dS) + \mathbf{f}_W + \mathbf{f}_I + \mathbf{f}_H = 0 \tag{1a}$$

Here, T' is the tension in the cable, S is the arc length measured along the cable, and $\mathbf{f}_W$, $\mathbf{f}_I$, and $\mathbf{f}_H$ are, respectively, the weight, inertial, and hydrodynamic loads per unit of cable length. Coupled to the equations of equilibrium must be added the geometric constraint

$$(d\mathbf{P}/dS \cdot d\mathbf{P}/dS)^{1/2} = 1 \tag{1b}$$

If S is taken as zero at the drogue end of the cable and as L at the towpoint, then the appropriate boundary condition at the towpoint is

$$\mathbf{P}(L) = R(\mathbf{i}\cos\theta_{tp} + \mathbf{j}\sin\theta_{tp}) + Z_{tp}\mathbf{k} \tag{2a}$$

where θ_{tp} is the angle which the towpoint makes with the reference X axis and where Z_{tp} is the Z coordinate of the towpoint. Both θ_{tp} and Z_{tp} are arbitrary, depending only on the choice of the reference coordinate system.

Equilibrium at the drogue end requires that

$$(T'd\mathbf{P}/dS)|_{s=0} + \mathbf{F}_d = 0 \tag{2b}$$

where $\mathbf{F}_d$ denotes the external force on the drogue referenced to the point of attachment of the cable.

The External Load on the Cable

If the linear density of the cable is given by μ, then the gravitational force per unit length is $-\mu g\mathbf{k}$ where g is the gravitational acceleration. Also, applying Archimedes' principle, the buoyancy force per unit length is $\rho A g\mathbf{k}$ where A is the cable cross-sectional area and ρ is the mass density of the towing medium. These forces combine to give the weight load $\mathbf{f}_W$ as

$$\mathbf{f}_W = -(\mu - \rho A)g\mathbf{k} \tag{3}$$

The inertial force $\mathbf{f}_I$ arises from the acceleration of the cable point $\mathbf{P}$ as seen by the fluid which is at rest. On remembering that in equilibrium the cable has no motion relative to the rotating coordinate system, this acceleration $\mathbf{a}$ is found from Coriolis' theorem as

$$\mathbf{a} = \Omega^2\mathbf{k} \times (\mathbf{k} \times \mathbf{P}) \tag{4}$$

The centripetal acceleration gives rise to a centrifugal load, $-\mu\mathbf{a}$, and also to an apparent mass load obtained from Lamb[4] as $-\rho A\mathbf{a}$. By adding these two forces and using Eq. (4), the inertial load per unit length becomes

$$\mathbf{f}_I = -(\mu + \rho A)\Omega^2\mathbf{k} \times (\mathbf{k} \times \mathbf{P}) \tag{5}$$

Consider now the hydrodynamic force. The usual method of specifying this force is to resolve it into components along three mutually perpendicular directions known as the hydrodynamic axes. These three directions are, respectively, parallel to the component of relative velocity which is normal to the cable, parallel to the component of relative velocity which is tangent to the cable, and parallel to the direction which is mutually orthogonal to the former two directions. In this coordinate system, the components of the hydrodynamic force are known, respectively, as the normal drag, the tangential drag, and the side drag. The relative velocity is the total velocity of the cable as seen in the rest frame of the fluid. Since, for the problem under consideration, the fluid is already at rest, the relative cable velocity $\mathbf{v}$ is given by

$$\mathbf{v} = \Omega\mathbf{k} \times \mathbf{P} \tag{6}$$

A number of researchers (see Ref. 5 for a complete bibliography) have discussed the forms and magnitudes of the drag components. Their results show that the effects of side and tangential drag on the equilibrium cable shape are usually negligible compared with the normal drag effects. Consequently, for the purposes of this paper, the side and tangential components of drag are set equal to zero. The hydrodynamic force then consists entirely of its normal drag component. If $\mathbf{v}_n$ is used to represent the component of relative velocity which is normal to the cable, the magnitude of the normal drag is known to be $(\frac{1}{2})\rho C_D d|\mathbf{v}_n|^2$, where d is the cable diameter and C_D is the cable drag coefficient. Since the normal drag acts to resist the normal motion of the cable, its direction of action is given by $-\mathbf{v}_n/|\mathbf{v}_n|$. The hydrodynamic force per unit length $\mathbf{f}_H$ is thus obtained as

$$\mathbf{f}_H = -(\tfrac{1}{2})\rho C_D d|\mathbf{v}_n|\mathbf{v}_n \tag{7a}$$

Further, since the unit tangent to the cable is given by $d\mathbf{P}/dS$, the normal and total velocities of the cable are related through the equation

$$\mathbf{v}_n = \mathbf{v} - (\mathbf{v}\cdot d\mathbf{P}/dS)d\mathbf{P}/dS \tag{7b}$$

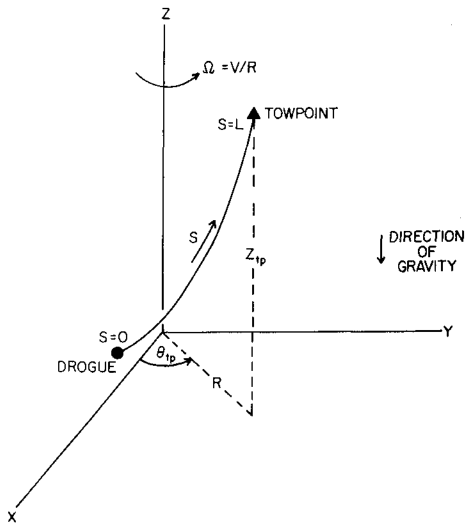

Fig. 1 Rotating coordinate system and notation.

which, by using Eq. (6) becomes

$$\mathbf{v}_n = \Omega\mathbf{k} \times \mathbf{P} - \Omega[(\mathbf{k} \times \mathbf{P})\cdot d\mathbf{P}/dS]d\mathbf{P}/dS \tag{7c}$$

In addition to neglecting the side and tangential components of drag, various other small effects such as cable extensibility, thermal strains, etc., have also been ignored. However, if one desires, these are easily included in the equilibrium problem and their inclusion changes neither the method of solution or the interpretation of the results. Their importance as parameters will become apparent only when accurate experiments are compared with numerical results. In this paper, the basic physical phenomena governing the equilibrium cable configuration are of primary interest, and these added small effects are conveniently forgotten.

The External Force on the Drogue

The evaluation of $\mathbf{F}_d$ implies a considerable knowledge about the physical and hydrodynamic characteristics of the drogue vehicle including the exact point of cable attachment. Although the problem is straightforward (see Ref. 6), the actual evaluation in terms of vehicle parameters is beyond the scope of this work. Rather, our attention will be restricted to a simple spherical drogue. Note again, however, that the inclusion of a more complex vehicle effects neither the method of solution or the interpretation of the results.

For the spherical drogue, there are no hydrodynamic moments present and, thus, the force at the point of attachment is equivalent to the force at the center of the sphere. By following the reasoning used in deriving the cable forces, the weight force $\mathbf{F}_{dW}$ becomes

$$\mathbf{F}_{dW} = -(W - W')\mathbf{k} \tag{8a}$$

where W is the drogue weight and W' is the weight of the displaced fluid. Similarly, the inertial force $\mathbf{F}_{dI}$ is

$$\mathbf{F}_{dI} = -(M + M')\Omega^2\mathbf{k} \times (\mathbf{k} \times \mathbf{P}_d) \tag{8b}$$

where M is the mass of the drogue, M' is the apparent mass of the drogue, and $\mathbf{P}_d$ is the position vector of the point of attachment to the drogue. The hydrodynamic load $\mathbf{F}_{dH}$ for a spherical drogue is readily obtained as

$$\mathbf{F}_{dH} = -(\tfrac{1}{2})\rho C_{Dd}A_d|\mathbf{v}_d|\mathbf{v}_d \tag{8c}$$

where C_{Dd} and A_d are, respectively, the coefficient of drag and the reference cross-sectional area of the drogue. The drogue velocity $\mathbf{v}_d$ is obtained from Eq. (6) as

$$\mathbf{v}_d = \Omega\mathbf{k} \times \mathbf{P}_d$$

A Nondimensional Form for the Circular Towing Problem

To determine the important combinations of parameters that appear in the circular towing problem, it is necessary to nondimensionalize the equilibrium equations and boundary conditions. Essentially, for a given cable and a given drogue, there are three quantities—the cable length L, the towpoint radius R, and the towpoint velocity V—which can be independently varied. The nondimensionalization chosen here, though not the simplest, does isolate the fixed from the independent parameters. Further, it readily indicates the modeling properties of the problem.

To obtain this nondimensionalization, all lengths are divided by R and the cable tension is divided by $(\mu + \rho A)gR$. With these definitions, the dimensionless arc length s, position vector $\mathbf{p}$, and tension T become

$$s = S/R \quad \mathbf{p} = \mathbf{P}/R \quad T = T'/[(\mu + \rho A)gR] \tag{9a}$$

Similarly, the dimensionless coordinates x, y, and z of the cable point s are related to the dimensional coordinates by

$$x = X/R \quad y = Y/R \quad z = Z/R \tag{9b}$$

After substituting these dimensionless quantities into Eq. (1a) and replacing the external cable forces by Eqs. (3, 5, and 7a), the complete static equilibrium equation becomes

$$d/ds(Td\mathbf{p}/ds) - w\mathbf{k} - \gamma^2\delta\mathbf{k} \times (\mathbf{k} \times \mathbf{p}) - C\gamma^2|\mathbf{v}_n^*|\mathbf{v}_n^* = 0 \tag{10a}$$

where $\mathbf{v}_n^*$ is the nondimensional normal velocity obtained from Eq. (7c) as

$$\mathbf{v}_n^* = \mathbf{k} \times \mathbf{p} - [(\mathbf{k} \times \mathbf{p})\cdot d\mathbf{p}/ds]d\mathbf{p}/ds \tag{10b}$$

The dimensionless cable weight w, drag constant C, diameter δ, and velocity γ are defined by

$$w = (\mu - \rho A)/(\mu + \rho A) \tag{11a}$$

$$C = (\tfrac{1}{2})\rho C_D d^2/(\mu + \rho A) \tag{11b}$$

$$\delta = d/R \tag{11c}$$

$$\gamma = V/(gd)^{1/2} \tag{11d}$$

Note that w and C are characteristics of the particular cable being towed, while δ and γ are characteristics of the independent towpoint parameters.

Coupled to the equilibrium equation, the geometric constraint, Eq. (1b), becomes

$$(d\mathbf{p}/ds\cdot d\mathbf{p}/ds)^{1/2} = 1 \tag{12}$$

On substituting Eqs. (8a–8c) into Eq. (2b) and recalling that $\mathbf{P}_d \equiv \mathbf{P}(0)$, the boundary condition at the drogue end of the cable becomes

$$[Td\mathbf{p}/ds - w_d\delta\mathbf{k} - m_d\gamma^2\delta^2\mathbf{k} \times (\mathbf{k} \times \mathbf{p}) - C_d\gamma^2\delta|\mathbf{k} \times \mathbf{p}|(\mathbf{k} \times \mathbf{p})]_{s=0} = 0 \tag{13}$$

where the dimensionless drogue weight w_d, mass m_d, and drag constant C_d are defined by

$$w_d = (W - W')/[(\mu + \rho A)gd] \tag{14a}$$

$$m_d = (M + M')/[(\mu + \rho A)d] \tag{14b}$$

$$C_d = (\tfrac{1}{2})\rho C_{Dd}A_d/(\mu + \rho A) \tag{14c}$$

Note that w_d, m_d, and C_d are characteristics only of the given cable and the given drogue. For a more complex drogue, additional parameters may be needed to adequately characterize the vehicle. Note, however, that these parameters would depend only on the material and dimensional properties of the drogue and cable since the velocity field is characterized independently by γ.

At the towpoint, the boundary condition Eq. (2a) now reads

$$\mathbf{p}(\lambda) = \mathbf{i}\cos\theta_{tp} + \mathbf{j}\sin\theta_{tp} + z_{tp}\mathbf{k} \tag{15a}$$

where z_{tp} designates the dimensionless z coordinate of the towpoint and where the dimensionless cable length λ is defined by

$$\lambda = L/R \tag{15b}$$

Modeling Properties of the Circular Towing Problem

According to Wilson,[7] the mass per unit length of cable μ can be written as

$$\mu = (K_\mu/g)d^2$$

where K_μ is a constant representative of a class of cable construction. Similarly, the displaced mass of fluid per unit length can be expressed as

$$\rho A = (K_\rho/g)d^2$$

where K_ρ is again a constant representative of the class of cable.

On substituting these expressions into the parameters which characterize the cable-drogue system [Eqs. (11a, 11b, and 14a–c)], one obtains

$$w = (K_\mu - K_\rho)/(K_\mu + K_\rho) \tag{16a}$$

$$C = (\tfrac{1}{2})\rho g C_D/(K_\mu + K_\rho) \tag{16b}$$

$$w_d = (W - W')/[(K_\mu + K_\rho)d^3] \tag{16c}$$

$$m_d = (M + M')g/[(K_\mu + K_\rho)d^3] \tag{16d}$$

$$C_d = (\tfrac{1}{2})\rho g C_{Dd}A_d/[(K_\mu + K_\rho)d^2] \tag{16e}$$

These equations show that both w and C are independent of the cable diameter d, depending only on the class of cable construction and the fluid density (through ρ and K_ρ). Also, if L_d represents a characteristic length of the drogue, then $(W - W')$, $(M + M')$, and A_d are respectively proportional to L_d^3, L_d^3, and L_d^2; and, consequently, w_d, m_d, and C_d depend only on the drogue, cable, and fluid materials and the quantity L_d/d. (As previously remarked, this statement would also be true for more complex drogues.) Thus, the proper modeling law for the parameters in Eqs. (16) is material equivalence and geometric similarity.

The remaining parameters δ, γ, and λ [Eqs. (11c, 11d, and 15b)] characterize the towpoint-cable system. If d_a, R_a, and V_a represent the actual cable diameter, towpoint radius, and towpoint velocity and if d_m, R_m, and V_m represent the modeling quantities, then equivalence of δ, γ, and λ between the two systems demands that

$$R_m = R_a(d_m/d_a) \tag{17a}$$

$$L_m = L_a(d_m/d_a) \tag{17b}$$

$$V_m = V_a(d_m/d_a)^{1/2} \tag{17c}$$

Equations (17a) and (17b) simply express geometric scaling, while Eq. (17c) expresses the scaling law for the normal hydrodynamic forces.

Equation (17), coupled with the modeling law for the cable-drogue parameters, yields the modeling law for the circular towing problem. Two circularly towed systems a and m are equivalent if they possess material and geometric similarity and if the velocities at the towpoints are related by $(V_m/V_a) = (d_m/d_a)^{1/2}$.

It is important to point out that this modeling law does not produce flow similarity. In fact, the relation between the model and actual Reynolds numbers at any point on the cable or at the drogue is

$$Re_m = Re_a(d_m/d_a)^{3/2}$$

However, if Reynolds number effects are unimportant (that is, essentially, if the side and tangential components of the hydrodynamic force are unimportant) and if both Re_a and Re_m remain in the range 10^2–10^5, then the model should produce reliable results. This conjecture must be validated by experiment. If the conjecture is incorrect, then a more detailed examination of the hydrodynamic forces must be made and, simultaneously, modeling becomes impossible.

Resultant Force Transformation

Since a numerical integration of the equilibrium equations is necessary, it is convenient to reduce them to a set of first-order differential equations. This is accomplished by the resultant force transformation defined as

$$d\mathbf{p}/ds = \boldsymbol{\tau}/T \tag{18a}$$

where $\boldsymbol{\tau}$ is the resultant force vector. On substituting Eq. (18a) into Eq. (12), the geometric constraint becomes the prognostic relation for the tension

$$T = (\boldsymbol{\tau}\cdot\boldsymbol{\tau})^{1/2} \tag{18b}$$

This substitution also reduces the equilibrium Eq. (10a) to the form

$$d\boldsymbol{\tau}/ds = w\mathbf{k} + \gamma^2\delta\mathbf{k} \times (\mathbf{k} \times \mathbf{p}) + C\gamma^2|\mathbf{v}_n^*|\mathbf{v}_n^* \tag{18c}$$

where, from Eq. (10b)

$$\mathbf{v}_n^* = \mathbf{k} \times \mathbf{p} - [(\mathbf{k} \times \mathbf{p})\cdot\boldsymbol{\tau}/T]\boldsymbol{\tau}/T \tag{18d}$$

Eqs. (18a) and (18c) represent six first-order differential equations for the six components of $\mathbf{p}$ and $\boldsymbol{\tau}$.

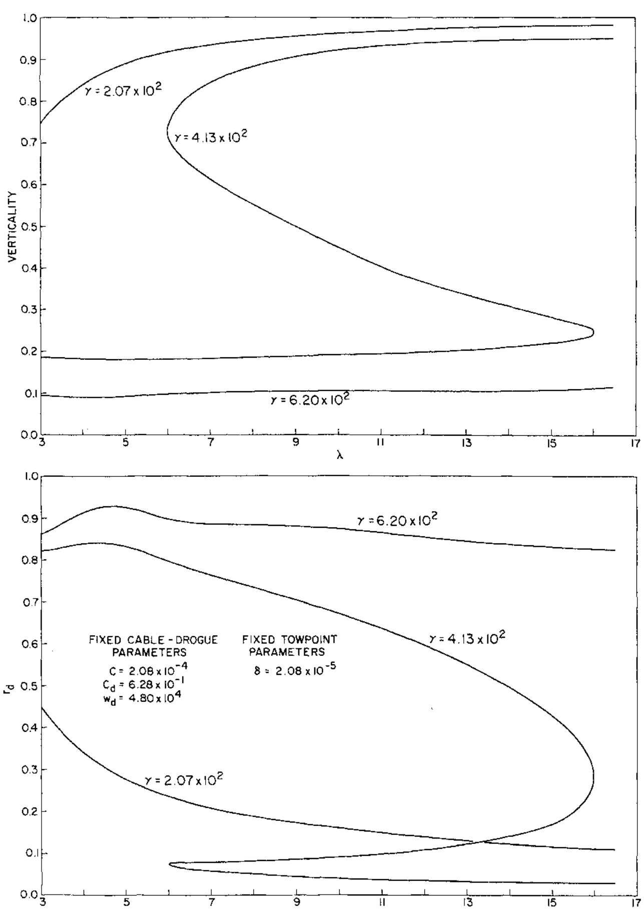

Fig. 2 Towline verticality and drogue radius r_d vs λ and γ for $\delta = 2.08 \times 10^{-5}$, $w_d = 4.80 \times 10^4$.

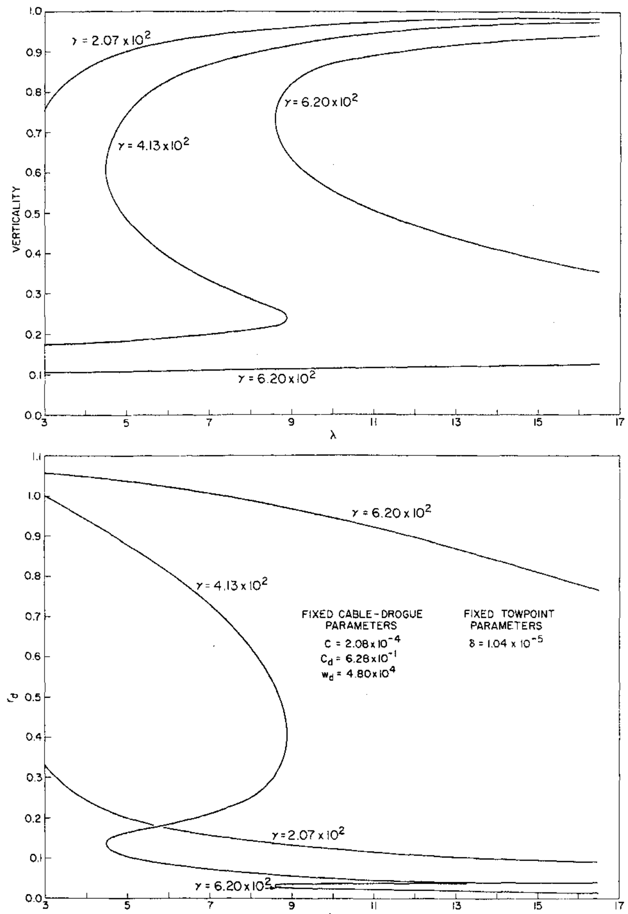

Fig. 3 Towline verticality and drogue radius r_d vs λ and γ for $\delta = 1.04 \times 10^{-5}$, $w_d = 4.80 \times 10^4$.

Method of Solution

Together with the boundary conditions at $s = 0$ and $s = \lambda$ [Eqs. (13) and (15a)], Eqs. (18a) and (18c) form a rather formidable nonlinear boundary value problem. Fortunately, by recognizing that Eqs. (18a) and (18c) are unaffected either by an arbitrary rotation about the z axis or by an arbitrary shift of the $z = 0$ reference plane, the boundary value problem can be converted into an initial value problem for which numerous numerical integration schemes exist. This is accomplished by choosing z_{tp} in a manner such that

$$z(0) \equiv 0 \tag{19a}$$

and by choosing θ_{tp} in a manner such that

$$y(0) \equiv 0 \tag{19b}$$

$$x(0) \equiv r_d \tag{19c}$$

The dimensionless equilibrium radius of the drogue r_d is taken to be a positive number.

With this choice of coordinates, the boundary condition at the drogue end of the cable, Eq. (13), becomes

$$\boldsymbol{\tau}(0) = w_d\delta\mathbf{k} - m_d\gamma^2\delta^2 r_d\mathbf{i} + C_d\gamma^2\delta r_d^2\mathbf{j} \tag{20}$$

Once r_d is specified, Eqs. (19) and (20) provide initial values for the integration of the equilibrium equations.

The method of solution now consists of guessing a value for r_d and integrating the equilibrium equations from $s = 0$ to $s = \lambda$. (In this paper, the fourth-order Runge-Kutta method has been used to perform the integration, and all calculations have been done with the cable length divided into 100 equal segments.) The guessed value of r_d is correct when the boundary condition at the towpoint $s = \lambda$, Eq. (15a), is satisfied.

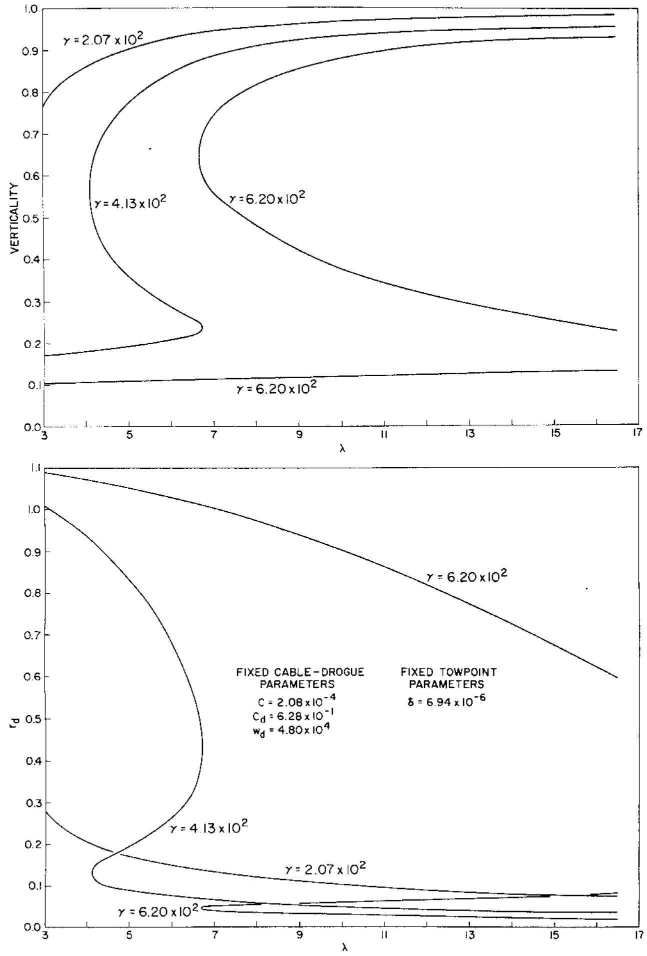

Fig. 4 Towline verticality and drogue radius r_d vs λ and γ for $\delta = 6.94 \times 10^{-6}$, $w_d = 4.80 \times 10^4$.

By the choice of initial value coordinates, this boundary condition becomes equivalent to

$$x^2(\lambda) + y^2(\lambda) = 1 \tag{21}$$

Note that geometric considerations for an inextensible cable bound the possible equilibrium values of r_d to the ranges

$$0 < r_d \leqq 1 + \lambda \qquad \text{for } \lambda \geqq 1$$

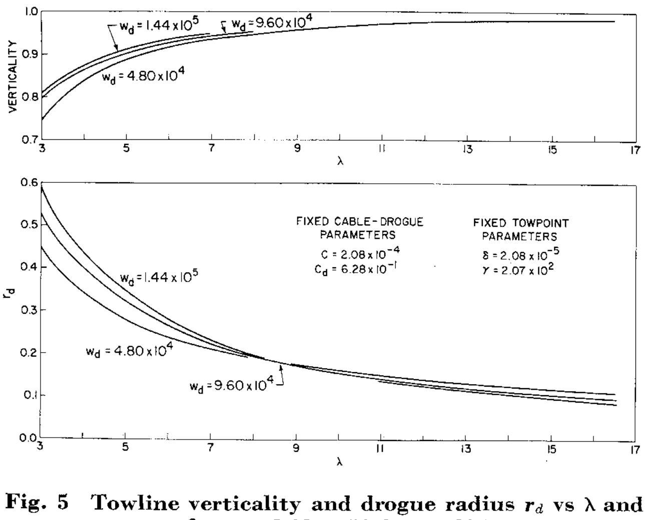

Fig. 5 Towline verticality and drogue radius r_d vs λ and w_d for $\delta = 2.08 \times 10^{-5}$, $\gamma = 207$.

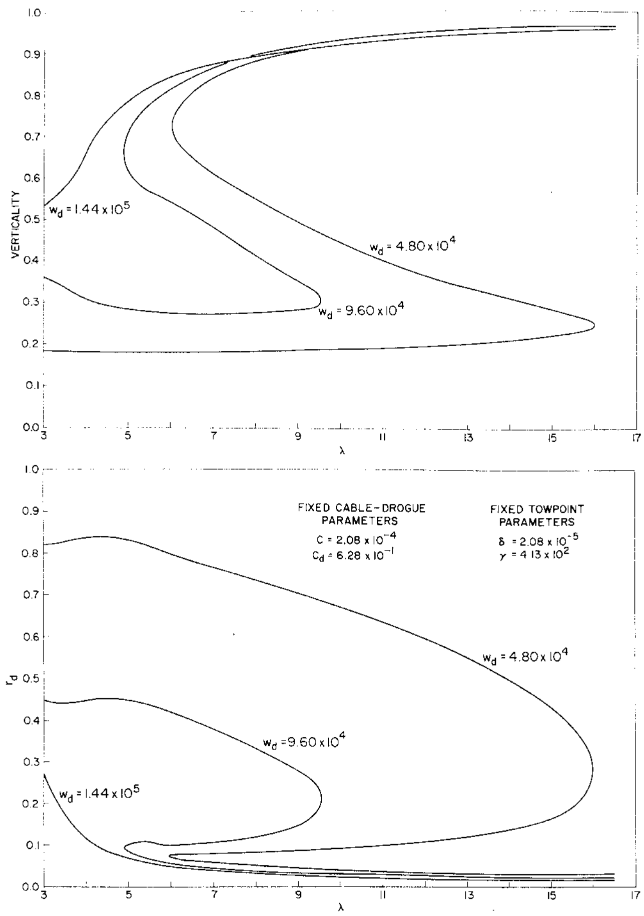

Fig. 6 Towline verticality and drogue radius r_d vs λ and w_d for $\delta = 2.08 \times 10^{-5}$, $\gamma = 413$.

and

$$1 - \lambda \leqq r_d \leqq 1 + \lambda \qquad \text{for } \lambda < 1$$

so that the search for r_d can be localized.

An Example: Pinpoint Deliveries from Fixed-Wing Aircraft

One of the more interesting aspects of the circular towing problem is that, for certain values of the governing parameters, the drogue obtains an equilibrium position very near the axis of rotation. The small value of r_d is also accompanied by a large verticality of the towline. This combination of small drogue radius and large verticality gives rise to several practical applications of the circular towing concept.

In this example, the pinpoint delivery of payloads from a fixed-wing aircraft flying in a circular pattern is examined. Since the system is airborne, it is permissible to neglect added mass and buoyancy effects; consequently, $K_\rho = 0$, $W' = 0$, and $M' = 0$. On referring to the fixed cable-drogue parameters in Eq. (16), this gives

$$w = 1$$

and

$$m_d = w_d$$

since the drogue weight W is identical to Mg.

To determine typical values for the remaining cable-drogue parameters, a system consisting of a $\frac{1}{4}$ in. steel cable and a 1 ft radius drogue weighing from 100 to 300 lb is considered. The value of K_μ is obtained from Wilson[7] as 1.60 lb/in.^{3}, and a value of 1.2 is taken as the drag coefficient of the cable. By

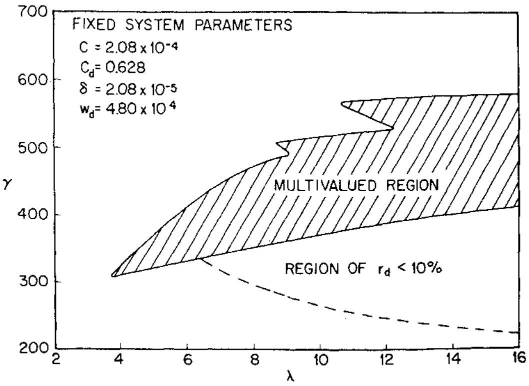

Fig. 7 Multivalued solution region as a function of λ and γ for $\delta = 2.08 \times 10^{-5}$, $w_d = 4.80 \times 10^4$.

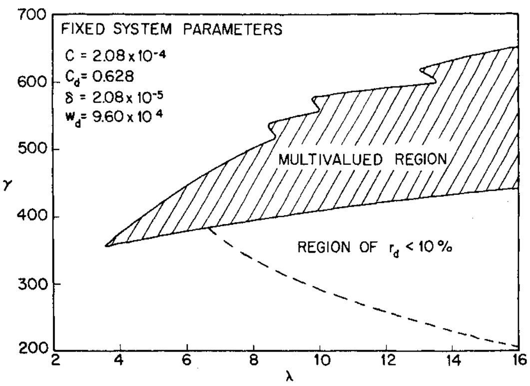

Fig. 8 Multivalued solution region as a function of λ and γ for $\delta = 2.08 \times 10^{-5}$, $w_d = 9.60 \times 10^4$.

using a drag coefficient of 0.5 for the spherical drogue, the remaining constants which characterize the system can be calculated as

$$C = 2.08 \times 10^{-4}$$

$$C_d = 0.628$$

$$w_d = 4.80 \times 10^4 \text{ to } 1.44 \times 10^5$$

The towplane is assumed to travel at from 100–300 knt in circles of from 1000–3000 ft radii. This yields typical towpoint parameters δ and γ [Eqs. (11c) and (11d)] as

$$\delta = 2.08 \times 10^{-5} \text{ to } 6.94 \times 10^{-6}$$

and

$$\gamma = 207 \text{ to } 620$$

Before discussing the results of the numerical calculations, recall that they are valid for any system which possesses material and geometric similarity to the above system and which satisfies the velocity scaling law Eq. (17c). Thus, for example, the effects of increasing γ [Eq. (11d)] for fixed C, C_d, w_d, and δ are equivalent to an increase in the towpoint velocity for the $\frac{1}{4}$ in. cable system, or a geometrically reduced system moving at the initial velocity, or various combinations of the former two cases. Similarly, the effects of decreasing δ [Eq. (11c)] for fixed C, C_d, w_d, and γ are equivalent to an increase in the towpoint radius for the $\frac{1}{4}$ in. cable system, or a geometrically smaller cable-drogue system moving at the initial radius but with reduced velocity, or various combinations of the former two cases.

Discussion of the Results

In Fig. 2, the towline verticality (z_{tp}/λ) and the equilibrium drogue radius are shown as functions of λ and γ for values of $\delta = 2.08 \times 10^{-5}$ and $w_d = 4.80 \times 10^4$. For $\gamma = 207$, the solution is seen to be unique for the considered range of λ. Further, as λ increases, the verticality asymptotically approaches a high value (approximately 98%) while, simultaneously, r_d approaches a small value (10%) of the towpoint radius. As γ increases to 413, the behavior of the solution changes radically, becoming multivalued for $6 < \lambda < 16$. Below $\lambda = 6$, it is impossible to obtain pinpoint deliveries since r_d is greater than 80% of the towpoint radius. However, above $\lambda = 16$, the verticality and drogue radius again asymptotically approach large and small values, respectively. In fact, the asymptotic value of $r_d = 3\%$ for $\gamma = 413$ is considerably less than the asymptotic value of 10% for $\gamma = 207$, although the verticality for the latter case is larger than that for the former. At present, little is known about the system response in the multivalued solution region, and this remains an outstanding area for study. As γ increases further to 620, the solution again becomes single valued, but now yields large r_d and very small verticality.

In Fig. 3, the effects of decreasing δ to 1.04×10^{-5} are plotted, again for a value of $w_d = 4.80 \times 10^4$. As in the previous figure, the solution for $\gamma = 207$ is unique; and the verticality and drogue radius approach, respectively, large and small values with increasing λ. As γ increases to 413, the solution again becomes multivalued for $4.50 < \lambda < 8.60$, and for $\lambda > 8.60$ pinpoint deliveries become possible. A similar statement is true for $\gamma = 620$. Note that the asymptotic value of r_d decreases as γ increases.

From Figs. 2 and 3, it can be concluded that in order to make pinpoint deliveries by flying in a circular pattern it is necessary (for fixed δ and w_d) to either have a γ value below the minimum value for which multivalued solutions exist or else, if γ is above this minimum value, to have a cable length λ larger than the upper bound of the multivalued region. These conclusions are verified in Fig. 4 where δ has been reduced to 6.94×10^{-6} while w_d remains at 4.80×10^4.

In Figs. 5 and 6, the effects of increasing the drogue weight w_d while holding the other parameters constant is considered. For $\gamma = 207$ and $\delta = 2.08 \times 10^{-5}$ (Fig. 5), it is seen that one effect of increasing w_d is to slightly lower the asymptotic value of r_d and to slightly increase the asymptotic value of the towline verticality. At $\gamma = 413$ and again for $\delta = 2.08 \times 10^{-5}$ (Fig. 6), the same effect on the asymptotic values is noted. In addition, an increase in the drogue weight shrinks the multivalued region, thus making it possible to obtain pinpoint deliveries with shorter lengths of cable.

The importance of knowing the multivalued regions of solution for fixed δ and w_d in order to ascertain the regions of small r_d and large verticality has already been alluded to. In Figs. 7, 8, and 9, these regions are shown as functions of λ and γ for increasing values of w_d and $\delta = 2.08 \times 10^{-5}$. Both the multivalued solution regions and the regions where r_d is

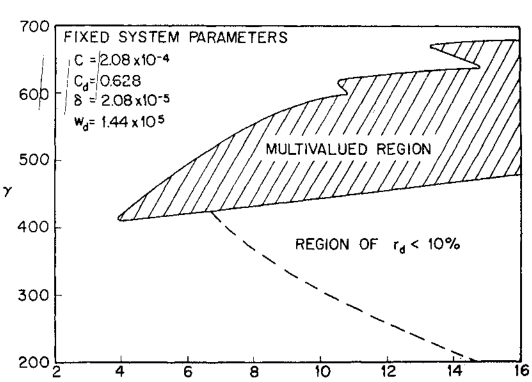

Fig. 9 Multivalued solution region as a function of λ and γ for $\delta = 2.08 \times 10^{-5}$, $w_d = 1.44 \times 10^5$.

simultaneously less than 10% and single valued are identified. Note that the primary effect of increasing w_d is an upward shift of the multivalued region along the γ axis.

Conclusions

The problem of predicting the configuration of a cable-drogue system towed in a steady circular path has been re-examined in this paper, and several outstanding research topics have been identified. First, under the assumptions of negligible side and tangential drag forces on the cable, a modeling law for the circular towing problem becomes possible. This law, however, does not preserve flow similarity and its validity must be experimentally determined. Second, for certain ranges of the parameters which govern the problem, the equilibrium solution is multivalued. Little is known about the system response in this multivalued region and the resolution of the behavior there is a question of both mathematical and physical interest.

The primary application of the circular towing concept is in the pinpoint delivery of payloads from fixed-wing aircraft or ships. For the fixed-wing aircraft, this paper has demonstrated an intimate relation between the multivalued regions of solution and the pinpoint delivery regions. Whether or not such a relation holds for the ship problem, where vastly different operating parameters exist, remains to be determined.

References

[1] Huang, J., "Mathematical Model for Long Cable Towed by Orbiting Aircraft," Rept. NADC-AM-6849, June 1969, U.S. Naval Air Development Center, Johnsville, Pa.

[2] Choo, Y., "Analytical Investigation of the Three-Dimensional Motion of Towed Systems," Ph.D. dissertation, June 1970, The Catholic Univ. of America, Washington, D.C.

[3] Skop, R., "On the Shape of a Cable Towed in a Circular Path," Rept. 7048, April 1970, U.S. Naval Research Lab., Washington, D.C.

[4] Lamb, H., *Hydrodynamics*, 6th ed., Dover, New York, 1945.

[5] Casarella, M. J. and Parsons, M., "Cable Systems under Hydrodynamic Loading," *Marine Technology Society Journal*, Vol. 4, No. 4, July-Aug. 1970, pp. 27–44.

[6] Strandhagen, A. G. and Thomas, C. F., "Dynamics of Towed Underwater Vehicles," Rept. 219, Nov. 1963, U.S. Navy Mine Defense Lab., Panama City, Fla.

[7] Wilson, B. W., "Elastic Characteristics of Moorings," *Journal of the Waterways and Harbors Division*, American Society of Civil Engineers, Vol. 93, No. WW4, Nov. 1967, pp. 27–56.

NOVEMBER 1971 J. AIRCRAFT VOL. 8, NO. 11

The Pilot Interface in Area Navigation

C. A. FENWICK, AND H. M. SCHWEIGHOFER*
Collins Radio Company, Cedar Rapids, Iowa

In order to realize the potential advantages of area navigation, the pilot's interface with the system must provide good visibility of the current navigation situation, of the preprogrammed flight plan, and of the system status. It must also permit efficient access for manual changes of the flight plan, utilizing stored data and automated processes insofar as practical to minimize the pilot workload. A control and display unit which provides such a pilot interface is described. It utilizes an alphanumeric display compatible with ATC procedures and a unique form of time-shared controls with logical branching to relevant display data.

Introduction

AREA navigation promises to increase the capacity of ordered airspace. It should also decrease the work load on air traffic controllers by reducing the need for radar vectoring. The increase in complexity of the air traffic route structure will be accompanied by an increase in the constraints imposed upon navigation in vertical and time dimensions as well.

On the surface, it might appear that increasing the number of airways and returning navigation responsibility to the cockpit could decrease pilot work load because voice communications with ATC could be reduced, requirements for heading changes could be anticipated well in advance, geographic location would be known (which is not always true with radar vectoring), and operations in holding patterns might occur less frequently. Similarly, it might appear that automation of navigation switching functions, such that a prestored flight plan could be executed entirely without pilot intervention, would be a major step toward elevating the pilot's role to that of flight manager. Nevertheless, tests to date have indicated that neither area navigation nor automation per se is a panacea for pilot work load problems; in fact, there is an inherent possibility that an inadequate pilot interface with the area navigation system can lead to a substantial increase in pilot work load with a resulting decrease in safety margin. The prevalent opinion that area navigation creates a need for a map display in the cockpit is evidence that this possibility is recognized, but the map display's virtues in facilitating geographic orientation do not seem to relate crucially to the question of over-all pilot work load, much of which involves data input tasks.

The purpose of this paper is to describe the underlying principles and illustrate the approach taken by Collins Radio Company toward reconciling the apparently conflicting requirements for decreasing pilot work load, increasing the complexity of airborne navigation functions, increasing pilot awareness of the navigation situation, and providing efficient access for manual inputs to processes which are largely automated.

Cockpit Information Flow

Basically, the problems appear to us to call for a major reappraisal of the organization of cockpit information flow

Presented as Paper 70-1335 at the AIAA Seventh Annual Meeting and Technical Display, Houston, Texas, October 19–22, 1970; submitted October 9, 1970; revision received June 1, 1971.

Index categories: Aircraft Flight Operations; Aircraft Subsystem Design.

* Research/Human Factors Technical Staff, Avionics Systems Division.